AIP | Review of Scientific Instruments

Manually operated scratch tester for characterization of mechanical properties of thin films

Hairong Wang, Chung Wo Ong, Yun Cheong Tsui, and Woon Ming Lau

Citation: Rev. Sci. Instrum. **76**, 016101 (2005); doi: 10.1063/1.1834706
View online: http://dx.doi.org/10.1063/1.1834706
View Table of Contents: http://rsi.aip.org/resource/1/RSINAK/v76/i1
Published by the American Institute of Physics.

Manually operated scratch tester for characterization of mechanical properties of thin films

Hairong Wang
Department of Applied Physics and Materials Research Center, Hong Kong Polytechnic University, Hung Hom, Kowloon, Hong Kong, People's Republic of China and School of Mechanical Engineering, Xi'an Jiaotong University, Xi'an, Shaanxi Province, People's Republic of China

Chung Wo Ong[a)]
Department of Applied Physics and Materials Research Center, Hong Kong Polytechnic University, Hung Hom, Kowloon, Hong Kong, People's Republic of China

Yun Cheong Tsui
Hong Kong Productivity Council, 78 Tat Chee Avenue, Kowloon Tong, Kowloon, Hong Kong, People's Republic of China

Woon Ming Lau
Department of Physics, The Chinese University of Hong Kong, Shatin, Hong Kong, People's Republic of China

(Received 10 March 2004; accepted 25 October 2004; published online 23 December 2004)

Based on the assumption that the results of a scratch test would not be affected significantly by some degree of variations of the rising rate of normal load and the speed of scratching, a manually operated scratch tester was developed for investigating the adhesion properties of coatings. The system can detect the friction force and normal load generated during a test, and identify the critical normal load L_c where the friction force becomes unstable. Measurements were made on glass, zirconium nitride coatings and aluminum oxide coatings for examining the reliability of the system. L_c of the three samples were 2.0 ± 0.41 N, 1.4 ± 0.32 N, and 0.52 ± 0.13 N. Results show that the system is good enough to serve as an economical replacement for a conventional scratch tester. [DOI: 10.1063/1.1834706]

I. INTRODUCTION

Scratch tests become popular in industries for monitoring the adhesion properties of coatings. In a scratch test, a diamond stylus is driven over a surface, with the normal load controlled by some units.[1–5] The critical load L_c of a coating, defined as the normal load at which catastrophic damage initiates, is determined from the test according to some guidelines, e.g., the point where the friction force becomes unstable. Although the failure may involve complicated mechanisms such as chipping, flaking, and cracking, L_c is still regarded as a useful adhesion indicator of a coating on a substrate.[6–9] Results facilitate comparisons of the adhesion properties between different coatings. A broad spectrum of scratch testers is already commercially available, where the load is made to cover a range from 10 μN to 200 N. Most systems are equipped with motor-driven translation stages for precision control of loading and scratching, where sophisticated sensors are employed for precision detection of friction force, normal load, displacement, and/or acoustic emission. However, we suggest that some components may not be necessary. First, acoustic sensors could be omitted because friction force detection is already sensitive enough to identify the initiation of failure.[10] Second, the variations of loading rate[5] and scratching speed do not significantly affect the detected value of L_c,[11] so the two parameters do not necessarily need to be controlled very stably and accurately in a scratch test. Based on these considerations, we established an economical and manually operated scratch tester, which had the function of recording real-time variations of normal load and friction force in a scratch test. In this paper, we report the configuration of the system, and the results of trial runs made on glass, zirconium nitride coatings (Zr–N) and aluminum oxide (Al–O) coatings deposited on 316 stainless steel (SS) by making use of the system.

II. INSTRUMENTATION AND EXPERIMENTAL DETAILS

A. Mechanical design

The mechanical parts of the scratch tester (Fig. 1) include a diamond ball tip (1, radius = 22 μm), two strain

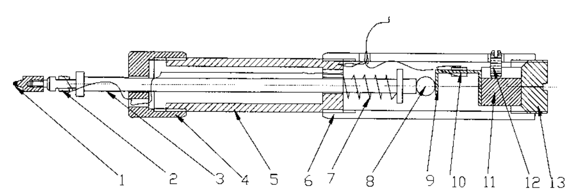

FIG. 1. Structure of the scratch tester: diamond ball tip (1), strain gauges for friction force detection (2), shaft (3), supporting parts (4–6), spring (7), steel ball (8), SS plate (9), strain gauges for normal load detection (10), sliding block (11), tightening screw and nut (12, 13).

[a)]Author to whom correspondence should be addressed; electronic mail: apacwong@inet.polyu.edu.hk

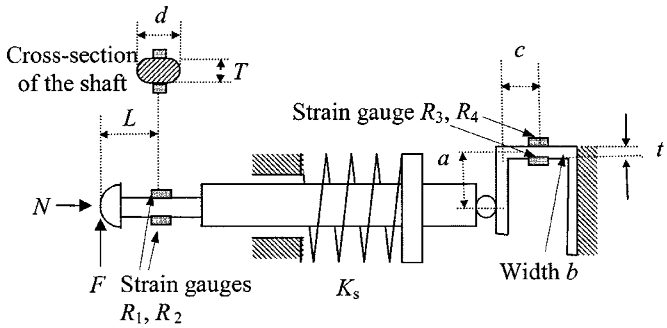

FIG. 2. Normal load and friction force detection units.

gauges for friction force detection (2), shaft (3), supporting parts (4–6), spring of 32 mm long and a force constant of 2500 N m^{-1} (7), steel ball (8), SS plate (9), two strain gauges for normal load detection (10), sliding block (11), tightening screw and nut (12 and 13). The strain gauges were from Tokyo Sokki Kenkyujo Co., Ltd. (Model No. TML FLK-1-17), with a resistance of 120 Ω and a gauge factor $G=2.17$. Voltage signals are generated by normal load and friction force, and are amplified by a circuit. The design has a full range of 10 N. Parts 12 and 13 are tightened to preload the steel plate (9).

It must be ensured that all critical parts would not experience stresses exceeding the yield stresses of the construction materials. First, the strains on the surface of shaft (3) where the strain gauges R_1 and R_2 are installed (Fig. 2) are $\varepsilon_1=N/EA+FL/EW_z$ and $\varepsilon_2=N/EA-FL/EW_z$. E is the elastic modulus, N the normal load, F the friction force, L the distance from the tip to the strain gauge (2), T the thickness, and d the width. A is the cross-sectional area $=(T/2)\sqrt{d^2-T^2}+(d^2/2)\arcsin(T/d)$, and $W_z=[(2T^2-d^2)/16]\sqrt{d^2-T^2}+(d^4/16T)\arcsin(T/d)$. By substituting $E=193$ GPa for 316 SS, $T=1$ mm, $d=4$ mm, $L=10$ mm, and the maximum N and $F=10$ N, the maximum strain is 800 μstrain. The maximum stress is thus determined to be 155 MPa, lower than the yield stress of 316 SS (205 MPa). Second, the strains on the surface of Part 9 where R_3 and R_4 are installed are $\varepsilon_3=N/EA_N+Na/EW_N$ and $\varepsilon_4=N/EA_N-Na/EW_N$. a is the dimension as shown in Fig. 2. A_N is the cross-sectional area bt. $W_N=bt^2/6$. t and b are the thickness and width. By substituting $a=5$ mm, $b=5$ mm, $t=0.7$ mm and $N=10$ N, the maximum strain is 650 μstrain. The maximum stress is thus determined to be 125 MPa, still below the yield stress of 316 SS.

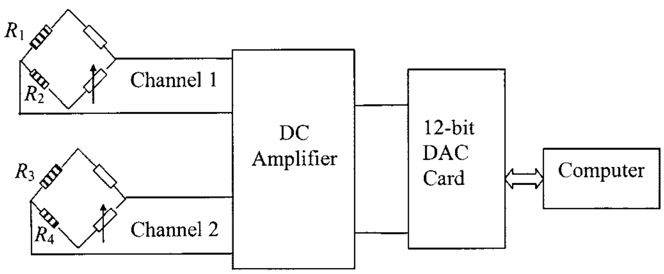

FIG. 3. Block diagram of the electrical circuit.

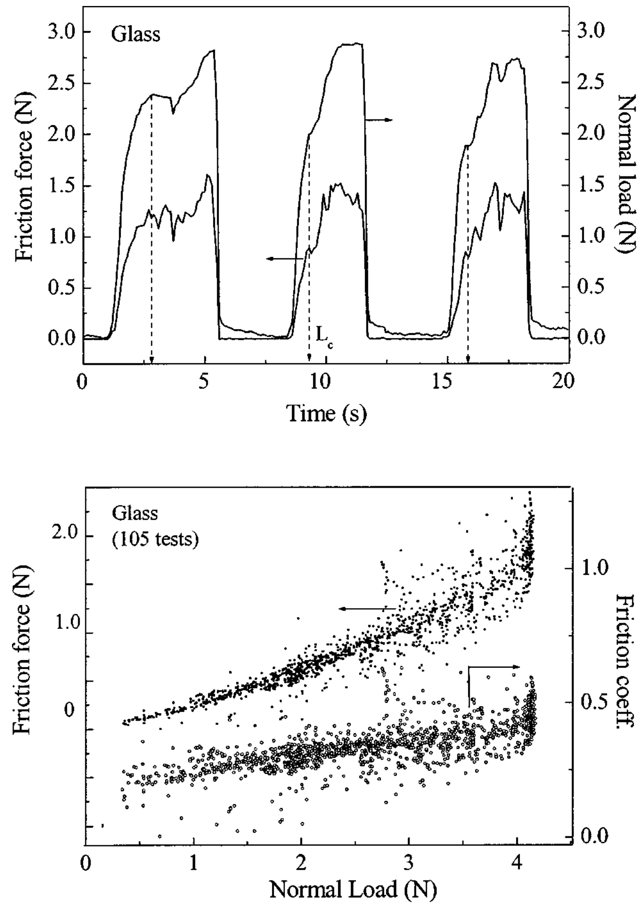

FIG. 4. Real-time profiles of friction force and normal load (upper), and the plots of friction force and friction coefficient vs normal load for 105 tests (lower) on glass.

B. Electrical design and data acquisition

Figure 3 shows the schematic diagram of the circuit. Strain gauges R_1 and R_2, and R_3 and R_4 form the arms of the two Wheatstone bridges. When one of R_1 and R_2 is under tensile stress, the other is under compressive stress. The voltage signals generated by the friction force and normal load are $(\varepsilon_1-\varepsilon_2)\times G=G(2FL/EW_z)$, and $(\varepsilon_3-\varepsilon_4)\times G=G(2Na/EW_z)$, respectively, where G is the gauge factor of the strain gauges. The signals are amplified by a two-channel dc amplifier, and then collected by a 12-bit DAC card (Advantech Co. Ltd., model PCL-818HG) with a speed of 10 MHz. A C++ program was compiled for real-time data processing, which deduced and continuously displayed the normal load and friction force. Every 100 data points were averaged to suppress the influence of random noise.

C. Calibration, operation, and data analysis

The force detection units were then calibrated by adding standard weights along and perpendicular to the shaft, respectively. The two voltage signals were confirmed to response linearly to the loads applied in the two directions with correlation coefficients equal to 0.9885 and 0.9831, respectively. The conversion factors were determined to be 4.8756 N V^{-1} and 2.333 N V^{-1}.

TABLE I. Results of scratch tests on glass, Zr–N coatings, and Al–O coatings on 316 SS.

	Thickness (μm)	No. of tests	Mean (N)	S.D. (N)	Load range (N)	Friction coeff.
Glass	···	105	2.0	0.41	0.98–2.9	0.33
Zr–N on SS	1.01	118	1.4	0.32	0.72–2.25	0.57
Al–O on SS	0.514	31	0.52	0.13	0.22–0.78	0.74

To perform a scratch test, the operator holds the device to scratch over the detected surface. The axis of the device is kept perpendicular to the sample surface. The normal load is increased gradually. Real-time profiles of normal load and friction force are thus produced and displayed. The friction coefficient is also deduced. The normal load at which the friction force profile starts to become unstable is regarded as L_c. Scattering of L_c obtained from repetitive measurements was observed, which may be due to the instability of manual operation and surface roughness, etc. However, random fluctuation of data can be suppressed by data processing technique. For example, our program has the function of removing unreasonable data based on the criterion proposed by Chauvenet.[12] Moreover, the mean of a population of data is used to serve as the estimate of L_c, and the standard deviation of the data set is referred to represent the error of the measurements.

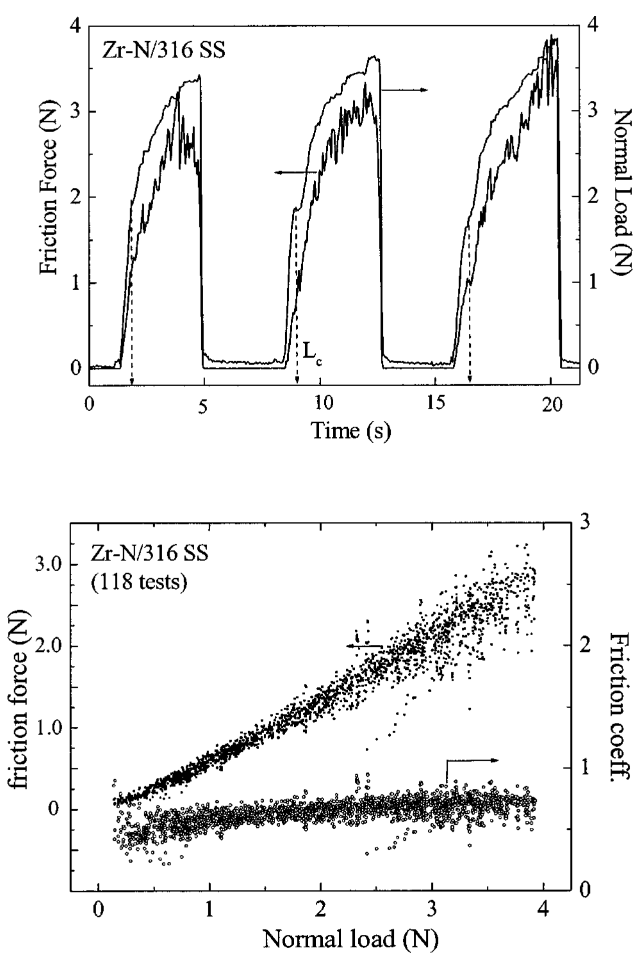

FIG. 5. Real-time profiles of friction force and normal load (upper), and the plots of friction force and friction coefficient vs normal load for 118 scratch tests (lower) on Zr–N coating deposited on 316 SS.

III. RESULTS AND DISCUSSION

Figure 4 (upper) shows the real-time profiles of friction force and normal load of several tests made on a glass slice. The friction force rose with increasing normal load first, and became very unstable when the load exceeded a certain level. The normal load corresponding to the appearance of the first kink is identified as the L_c value. Figure 4 (lower) shows the plots of friction force and friction coefficient vs normal load for 105 repetitive tests. Results showed that although the loading rate and scratching speed were loosely controlled, the distribution of the data points still exhibited a clear correlation with the applied load. This reflects the reproducibility of measurements made by the system. In addition, the friction coefficient of the glass-diamond couple can be estimated from the average of the data points in a certain load range. Scattering of data can be diminished by averaging the results of repetitive measurements. The mean value of L_c of 105 tests was determined to be 2.4 N, which was used as the estimate of the critical load of glass. The error was reflected by the standard deviation of the data set, which was determined to be 0.41 N, equivalent to ±8.5%. The average friction coefficient in the load range concerned is 0.33. All these data are summarized in Table I.

Figure 5 (upper) shows the real-time profiles of friction force and normal load for a Zr–N coating deposited on 316 SS. The two parameters increased with load first, and then became unstable when the load exceeded a certain level. The load corresponding to the appearance of the fist kink was regarded as the L_c value of the coating. Figure 5 (lower) also shows the data of friction force and friction coefficient vs normal load collected from 118 tests. Each group of the data exhibits a clear normal load dependence. The mean of L_c of all the tests was 1.4 N, which was regarded as a good guess of the critical load of the coating. The standard deviation was 0.32 N, corresponding to a ±11% error. The average friction coefficient of the Zr–N coating-diamond couple in the load range of 0.72–2.25 N is 0.57. Finally, for Al–O coatings on 316 SS, the critical load, standard deviation and average friction coefficient in the load range of 0.22–0.78 N are 0.52 N, 0.13 N (or ±12.5% error) and 0.74.

ACKNOWLEDGMENTS

The work described in this paper was substantially supported by an internal grant of the Hong Kong Polytechnic University (account code: A-PE07), and an Innovation and Technology Fund under a project with a title of “A multi-institutional effort to establish an advanced surface technologies development center” (account Code: K.11.2A.ZP07).

[1] V. Bellido-González, N. Stefanopoulos, and F. Deguilhen, Surf. Coat. Technol. **74–75**, 884 (1995).
[2] W. Heinke, A. Leyland, A. Matthews, G. Berg, C. Friedrich, and E. Broszeit, Thin Solid Films **270**, 431 (1995).
[3] M. Maillat and H. E. Hintermann, Surf. Coat. Technol. **68–69**, 638 (1994).
[4] S. Miyake, S. Watanabe, M. Murakawa, R. Kaneko, and T. Miyamoto, Thin Solid Films **212**, 262 (1992).
[5] J. Valli, J. Vac. Sci. Technol. A **4**, 3007 (1986).
[6] P. J. Burnett and D. S. Rickerby, Thin Solid Films **157**, 233 (1988).
[7] S. J. Bull and D. S. Rickerby, Surf. Coat. Technol. **42**, 149 (1990).
[8] P. A. Steinmann and H. E. Hintermann, J. Vac. Sci. Technol. A **3**, 2394 (1985).
[9] B. Hammer and A. J. Perry, Thin Solid Films **96**, 45 (1982).
[10] J. Valli, U. Mäkelä, A. Matthews, and V. Murawa, J. Vac. Sci. Technol. A **3**, 2411 (1985).
[11] P. A. Steinmann, Y. Tardy, and H. E. Hintermann, Thin Solid Films **154**, 333 (1987).
[12] J. R. Taylor, *An Instruction to Error Analysis*, 2nd ed. (University Science Book, Sausalito, 1997), p. 166.